Journal of Statistical Physics, Vol. 118, Nos. 1/2, January 2005 (© 2005)
DOI: 10.1007/s10955-004-8775-7

Asymptotic Behavior of the Order Parameter in a Stochastic Sandpile

Ronaldo Vidigal[1] **and Ronald Dickman**[1]

Received May 25, 2004; accepted August 13, 2004

We derive the first four terms in a series for the order paramater (the stationary activity density ρ) in the supercritical regime of a one-dimensional stochastic sandpile; in the two-dimensional case the first three terms are reported. This is done by reorganizing the pertubation theory derived using a path-integral formalism [Dickman and Vidigal, J. Phys. A **35**, 7269 (2002)], to obtain an expansion for stationary properties. Since the process has a strictly conserved particle density p, the Fourier mode $N^{-1}\psi_{k=0} \to p$, when $N \to \infty$, and so is not a random variable. Isolating this mode, we obtain a new effective action leading to an expansion for ρ in the parameter $\kappa \equiv 1/(1+4p)$. This requires enumeration and numerical evaluation of more than 200,000 diagrams, for which task we develop a computational algorithm. Predictions derived from this series are in good accord with simulation results. We also discuss the nature of correlation functions and one-site reduced distributions in the small-κ (high-density) limit.

KEY WORDS: Sandpiles; series expansion; path integrals; stochastic processes; phase transitions.

1. INTRODUCTION

Sandpile models were introduced some 15 years ago as examples of self-organized criticality (SOC), or scale invariance in the apparent absence of adjustable parameters.[1–5] Although not directly related to real sand or other granular systems, these models have attracted great interest in the quest for understanding the ubiquity of power-law distributions in nature[6], for example in earthquakes.[7,8]

[1]Departamento de Física, ICEx, Universidade Federal de Minas Gerais, 30123-970 Belo Horizonte, Minas Gerais, Brazil; e-mail: rvidigal@dedalus.lcc.ufmg.br, dickman@fisica.ufmg.br

Subsequently the appearance of "spontaneous" criticality in sandpiles was shown to result from a control mechanism that forces the system to a critical point marking a phase transition to an absorbing state.[9–11] This absorbing-state phase transition is observed in sandpiles with the same local dynamics as the original self-organized versions, but with a strictly conserved particle density, p, which plays the role of a temperature-like control parameter. Sandpiles with a strictly conserved particle number (to be called "conserved sandpiles" in what follows) are not self-organized: to achieve criticality, the particle density must be adjusted to its critical value, just as the temperature must be adjusted in a fluid or magnetic system. The particle addition and loss rules in self-organized sandpiles amount to a control scheme that forces p to its critical value.[9]

Conserved sandpiles, as noted, exhibit an absorbing-state phase transition,[12–14] analogous to that of the contact process or directed percolation (DP). Although the DP universality class is generic for absorbing-state phase transitions,[15,16] simulation results suggest that conserved sandpiles belong to universality classes other than DP. The difference is commonly attributed to the presence of a conserved field (the particle density), but there is as yet no firm basis for this assertion. Understanding criticality in conserved sandpiles thus presents an interesting challenge to the ongoing program of understanding nonequilibrium universality classes.[12,13,17] For the stochastic sandpile to be studied here, simulation results yield larger values for the critical exponent β, associated with the order parameter, (about 0.39 and 0.64 in one and two dimensions, respectively), than the corresponding DP values (0.2765 and 0.583 in one and two dimensions). DP-like critical behavior has been established for sandpiles with "sticky grains" (in this case above-threshold sites do not always topple).[18] Finally, the Bak–Tang–Wiesenfeld model, with a deterministic toppling rule, appears to define its own universality class.[19,20] In the case of conserved sandpiles, a systematic renormalization group analysis using the epsilon expansion is as yet unavailable. In fact, even the value of the upper critical dimension remains controversial.[11,21–23] Conflicting critical exponent values have been reported for the one-dimensional stochastic conserved sandpile,[24–27] possibly reflecting finite-size effects.

Until now, most quantitative results for conserved sandpiles have been based on simulations,[19,24–26,28,29] an important exception being the solution by Priezzhev *et al.*[30] of a directed, conserved version of the Maslov–Zhang model[31] via the Bethe ansatz. Phenomenological field theories have been proposed for sandpiles,[11,21,22] but their analysis is far from straightforward. Given the conflicting simulation results in the literature regarding critical exponents for conserved stochastic sandpiles, it is of interest to develop alternative approaches. Series analysis has been one

of the most precise methods for studying critical behavior (both in and out of equilibrium) since its introduction roughly fifty years ago. Recently, a time-dependent perturbation theory based on a path-integral formalism was derived for a stochastic sandpile.[32] In ref. 33 this short-time expansion for the one-dimensional case was extended using operator methods. These studies, along with the present work, are part of an effort to extend series methods to sandpiles. Although the present results are not sufficient to yield precision estimates of critical parameters, we believe that this work represents an important step towards this goal. The theoretical and computational methods developed here are, moreover, applicable to other problems in nonequilibrium statistical physics.

In the present work, the perturbation theory developed in ref. 32 is reformulated, leading to a quite different result: an expansion for *stationary* ($t \to \infty$) properties in powers of a parameter $\kappa \equiv 1/(1+4p)$ (in other words, a *high-density* expansion), instead of the short-time expansion (with p-dependent coefficients) obtained previously. Since p is the temperature-like control parameter, with large p corresponding the active phase (nonzero order parameter), the expansion in powers of κ is analogous to a low-temperature expansion of an equilibrium model. We obtain the first four terms (three terms in the two-dimensional case) of the activity series, thereby providing the first analytical results for the stationary properties of the model.

Our analysis employs two basic tools. One is an operator formalism for Markov processes, of the kind developed by Doi,[34] which has been applied to various models exhibiting nonequilibrium phase transitions.[35–39] The second is an exact mapping, devised by Peliti, of a Markov process to a path-integral representation.[40,41] This approach is frequently used to generate the effective action corresponding to a process, for subsequent analysis via renormalization group (RG) techniques. In the present instance our immediate objective is not a RG analysis but an expansion for the order parameter. In the path-integral formalism the probability generating function is written in terms of functional integrals over the fields $\psi(x,t)$ (whose expectation is the particle density at site x), and an auxiliary field $\tilde{\psi}(x,t)$. Our reformulation of the effective action is based on the observation that, due to particle conservation, the Fourier mode $N^{-1}\psi_{k=0}$ is not a random variable, but rather converges to the fixed value p as N, the number of lattice sites, tends to infinity.

We consider Manna's stochastic sandpile in its particle-conserving version.[24,32,42,43] The configuration is specified by the occupation number n at each site; sites with $n \geqslant 2$ are said to be *active*, and have a positive rate of *toppling*. When a site topples, it loses exactly two particles ("grains of sand"), which move randomly and independently to

nearest-neighbor sites. (Any configuration devoid of active sites is *absorbing*, i.e., no futher evolution of the system is possible once such a configuration is reached.) In this work, as in,[32,33] we adopt a toppling rate of $n(n-1)$ at a site having n particles, which leads us to define the order parameter as $\rho = \langle n(n-1) \rangle$. This choice of rate represents a slight departure from the examples studied previously, in which all active sites have the same toppling rate. (In the latter case it is natural to define the order parameter as the fraction of active sites.) The present rate leads to a much simpler evolution operator, and, on the other hand, should yield the same scaling properties, since sandpiles, like critical phenomena in general, exhibit a high degree of universality. (Close to the critical point, the density of sites with $n \geqslant 3$ particles is quite low, so that in practical terms our choice of rate should not greatly alter quantitative properties. Since studies of *restricted-height* sandpiles[23,28] reveal that they belong to the same universality class as their unrestricted counterparts, there is good reason to expect that a small change in transition rates, which does not modify the symmetry or conservation laws of the model, will have no effect on critical exponents.) Preliminary simulation results indicate that the model studied here exhibits a continuous phase transition at $p_c = 0.9493$, in one dimension; this is quite close to the corresponding value, $p_c = 0.94885$, for the model in which all active sites have the same toppling rate.[24]

The balance of this article is organized as follows. In section 2 we give a systematic definition of the model, review the path-integral formalism, and discuss the reorganization of the action. In section 3 we develop the perturbation expansion for the activity density in the supercritical regime. section 4 presents the diagrammatic expansion rules and the computational algorithm used to enumerate and evaluate diagrams. Predictions for the activity density are reported and compared against simulation in section 5, while in section 6 we examine correlation functions and higher moments of the density. In section 7, we present a brief discussion of our results.

2. MODEL AND FORMALISM

2.1. Model

We consider Manna's stochastic sandpile in its particle-conserving version.[24,42,43] The model is defined on a ring or (in $d \geqslant 2$ dimensions) hypercubic lattice with periodic boundaries. The configuration is specified by the occupation number n at each site; sites having $n \geqslant 2$ are *active*, and have a toppling rate of $n(n-1)$. (There is no upper limit on the number of particles that may occupy a given site.) When a site i topples, two particles

jump from i to nearest-neighbor sites, randomly and independently. Initially, a certain number M of particles are placed on the N^d sites of the lattice. The particle density $p = M/N^d$ is conserved under the dynamics.

Various initial distributions are possible. As in refs. 32 and 33 we consider, for simplicity, a product-Poisson initial distribution with intensity p at each site. We note that for finite N, the fluctuations in particle density associated with this distribution may effectively mask the phase transition, since, even for $p < p_c$, there is a nonzero probability of having $M/N^d > p_c$. In the limit $N \to \infty$, which is implicitly taken here (and in refs. 32 and 33), $M/N^d \to p$, i.e., the particle density is sharply distributed. In simulation studies of sandpiles (including those reported below) one normally fixes $M = Np$ rather than using a Poissonian initial condition, to avoid fluctuations in the total density.

Let $\{n\} \equiv (n_1, n_2, ..., n_N)$ denote the set of occupation variables defining a configuration. Note that this is a Markov process with an infinite state space (even for N finite) since there is no upper limit on the total number of particles. The dynamics is defined by a set of transition rates $w(\{n'\}, \{n\})$ (from $\{n\}$ to $\{n'\}$) which are nonzero only if $\{n'\}$ differs from $\{n\}$ on a set of two or three sites (site i, say, and either one or two nearest neighbors of i), such that $n_i' = n_i - 2$ and the neighbor or neighbors gain a total of two particles. Specifically, in one dimension the nonzero transition rates are

$$w(\{n'\}, \{n\}) = \begin{cases} \frac{1}{4} n_i (n_i - 1) & \text{if } n_{i-1}' = n_{i-1} + 2 \text{ and } n_{i+1}' = n_{i+1}, \\ \frac{1}{4} n_i (n_i - 1) & \text{if } n_{i+1}' = n_{i+1} + 2 \text{ and } n_{i-1}' = n_{i-1}, \\ \frac{1}{2} n_i (n_i - 1) & \text{if } n_{i-1}' = n_{i-1} + 1 \text{ and } n_{i+1}' = n_{i+1} + 1. \end{cases} \tag{1}$$

Evidently, configurations $\{n\}$ in which $n_i < 2$, $\forall i$ are absorbing. Such configurations exist for $p \leqslant 1$. Simulation results nevertheless indicate that an active stationary state is possible for particle densities greater than p_c, where the critical density p_c is strictly less than unity.[2]

We write the master equation for the process in the form[40,41]:

$$\frac{d|\Psi\rangle}{dt} = L|\Psi\rangle,$$

[2]It is worth noting that a rigorous proof of a continuous phase transition at a $p_c < 1$ is so far lacking.

where

$$|\Psi\rangle = \sum_{\{n\}} p(\{n\}, t)|\{n\}\rangle$$

is the probability distribution. Here $p(\{n\}, t)$ is the probability of configuration $\{n\}$, and the state $|\{n\}\rangle$ is a direct product of states $|n_j\rangle$, representing exactly n_j particles at site j.[40]

Defining creation and annihilation operators via the relations,

$$a_i|n_i\rangle = n_i|n_i - 1\rangle$$

and

$$\pi_i|n_i\rangle = |n_i + 1\rangle,$$

the evolution operator for the one-dimensional stochastic sandpile, corresponding to the rates of Eq. (1), is

$$L = \sum_i \left[\frac{1}{4}(\pi_{i-1} + \pi_{i+1})^2 - \pi_i^2\right] a_i^2. \tag{2}$$

(For simplicity we begin the analysis in one dimension; the generalization to d dimensions is straightforward.) It is readily seen that L conserves the number of particles: two particles are removed from an active site i and transferred to either or both nearest neighbors.

2.2. Path-Integral Representation

To lay the groundwork for the perturbative analysis, we map the Markov process defined above to a path-integral representation. As explained in refs. 40 and 41, this involves the introduction of a probability generating function

$$\Phi_t(\{z\}) \equiv \sum_{\{n\}} p(\{n\}, t) \prod_j z_j^{n_j}, \tag{3}$$

(here $\{z\} = (z_1, z_2, ..., z_N)$ is shorthand for the set of generating function variables), and an "evolution kernel" $U_t(\{z\}, \{\zeta\})$. The latter is used to evolve the probability generating function, via[40],

$$\Phi_t(\{z\}) = \prod_j \int \frac{d\zeta_j d\zeta_j'}{2\pi} e^{-i\sum_j \zeta_j \zeta_j'} U_t(\{z\}, \{\zeta\}) \Phi_0(\{i\zeta'\}) \quad (t \geqslant 0), \tag{4}$$

where $\Phi_0(\{i\zeta'\})$ denotes the initial generating function $\Phi_0(\{z\})$ with arguments $z_j = i\zeta'_j$. (Here and below, integrals with limits unspecified are over the real axis unless otherwise stated.)

Now since L is in normal form (all operators π to the left of all operators a), we can immediately write down a path-integral expression for the evolution kernel, following Peliti's prescription[40,41]

$$U_t(\{z\},\{\zeta\}) = \int \mathcal{D}\hat{\psi}\mathcal{D}\psi \exp\left[-\int_0^t dt' \left\{ \sum_j \hat{\psi}_j \dot{\psi}_j + \sum_j \left[\frac{1}{4}(\hat{\psi}_{j-1} + \hat{\psi}_{j+1})^2 - \hat{\psi}_j^2\right]\psi_j^2 \right\} + \sum_j z_j \psi_j(t) \right], \quad (5)$$

with the boundary conditions $\psi_j(0) = \zeta_j$ and $\hat{\psi}_j(t) = z_j$. (The dot denotes a time derivative.) The functional integrals are over $\psi_j(s)$ and $\hat{\psi}_j(s)$ for $0 \leqslant s \leqslant t$:

$$\int \mathcal{D}\hat{\psi}\mathcal{D}\psi \equiv \prod_j \int \mathcal{D}\hat{\psi}_j \int \mathcal{D}\psi_j . \quad (6)$$

Given the initial product-Poisson distribution, we have,

$$\Phi_0(\{z\}) = \exp[p\sum_j (z_j - 1)]. \quad (7)$$

Noting that

$$\int \frac{d\zeta\, d\zeta'}{2\pi} f(\zeta) e^{i\zeta'(p-\zeta)} = f(p), \quad (8)$$

we see that for a Poisson initial distribution,

$$\Phi_t(\{z\}) = e^{-Np} U_t(\{z\};\{\zeta\})|_{\zeta_j = p}. \quad (9)$$

Thus the generating function at time t is e^{-Np} times the right hand side of Eq. (5), evaluated with $\psi_j(0) = \zeta_j = p$.

Let

$$U_t(\{z\},\{\zeta\}) = \int \mathcal{D}\hat{\psi}\mathcal{D}\psi\, \mathcal{G}'[\psi,\hat{\psi}], \quad (10)$$

where $\mathcal{G}'$ represents the exponential in Eq. (5), and let

$$\langle \mathcal{A} \rangle \equiv e^{-Np} \int \mathcal{D}\hat{\psi}\mathcal{D}\psi \; \mathcal{A}\,\mathcal{G}'[\psi, \hat{\psi}]\Big|_{z_n=1} , \tag{11}$$

where $\mathcal{A}$ is a function of the fields ψ and $\hat{\psi}$.

The simplest observables of interest are the mean occupation number (at site j),

$$\langle n_j \rangle = \left. \frac{\partial \Phi_t(\{z\})}{\partial z_j} \right|_{z_n=1} = \langle \psi_j \rangle , \tag{12}$$

and the mean activity,

$$\langle n_j (n_j - 1) \rangle = \left. \frac{\partial^2 \Phi_t(\{z\})}{\partial z_j^2} \right|_{z_n=1} = \langle \psi_j^2 \rangle . \tag{13}$$

Since the system is translation-invariant it is more convenient to study $\phi \equiv N^{-1} \sum_j \langle n_j \rangle$ and $\rho \equiv N^{-1} \sum_j \langle n_j (n_j - 1) \rangle$. (Note that $\phi = p$ is a constant of the motion, so this quantity serves principally as a check on our analysis.) We now introduce the discrete Fourier transform via

$$\psi_k = \sum_j e^{-ijk} \psi_j , \tag{14}$$

with inverse

$$\psi_j = \frac{1}{N} \sum_k e^{ijk} \psi_k , \tag{15}$$

(and similarly for other variables), where the allowed values of the wavevector are

$$k = -\pi, \; -\pi + \frac{2\pi}{N}, \ldots, -\frac{2\pi}{N}, \; 0, \; \frac{2\pi}{N}, \ldots, \pi - \frac{2\pi}{N} . \tag{16}$$

(To avoid heavy notation, we indicate the Fourier transform by the subscript k; the subscript j denotes the corresponding variable on the lattice.)

In the Fourier representation, the evolution kernel may be written

$$U_t(\{z\},\{\zeta\}) = \int \mathcal{D}\hat{\psi}\mathcal{D}\psi \exp\left[-\int_0^t dt' \left\{ N^{-1}\sum_k \hat{\psi}_k \dot{\psi}_{-k} + N^{-3}\sum_{k_1,k_2,k_3} \omega_{k_1,k_2}\hat{\psi}_{k_1}\hat{\psi}_{k_2}\psi_{k_3}\psi_{-k_1-k_2-k_3}\right\} + N^{-1}\sum_k z_k \psi_{-k}(t)\right], \tag{17}$$

where $\omega_{k_1,k_2} = 1 - \cos k_1 \cos k_2$, and the boundary conditions are $\psi_k(0) = \zeta_k$ and $\hat{\psi}_k(t) = z_k$. (The condition $z_j = 1$ for all sites corresponds to $z_k = N\delta_{k,0}$.) The functional integrals are over the ψ_k and $\hat{\psi}_k$ with k ranging over the first Brillouin zone, Eq. (16). The activity density takes the form

$$\rho(t) \equiv N^{-1}\sum_j \langle n_j(n_j - 1)\rangle = N^{-2}\sum_k \langle \psi_k \psi_{-k}\rangle, \tag{18}$$

while $\phi = N^{-1}\langle \psi_{k=0}\rangle$.

In the d-dimensional case, Eq. (17) remains valid if we let

$$\omega_{\mathbf{k_1},\mathbf{k_2}} = 1 - \lambda_d(\mathbf{k_1})\lambda_d(\mathbf{k_2}), \tag{19}$$

with

$$\lambda_d(\mathbf{k}) \equiv \frac{1}{d}\sum_{\alpha=1}^{d} \cos k_\alpha. \tag{20}$$

The wavevectors now range over the first Brillouin zone in d dimensions.

It is convenient at this point to perform a change of variables, letting $\tilde{\psi}_k = \hat{\psi}_k - N\delta_{k,0}$. As a result, $\mathcal{G}'$ gains a factor of e^{Np} (which cancels the prefactor in Eq. (11)), and the boundary term in the argument of the exponential vanishes when we set $z_k = N\delta_{k,0}$. Then we have,

$$\langle \mathcal{A}\rangle = \int \mathcal{D}\tilde{\psi}\mathcal{D}\psi\, \mathcal{A}\,\mathcal{G}[\psi,\tilde{\psi}], \tag{21}$$

where

$$\mathcal{G}[\psi,\tilde{\psi}] \equiv \exp\left[-N^{-1}\int_0^t dt' \sum_k \tilde{\psi}_k \dot{\psi}_{-k} + \int_0^t dt' \mathcal{L}_I\right], \tag{22}$$

and where the "interaction" is now

$$\mathcal{L}_I = -N^{-3} \sum_{k_1,k_2,k_3} \omega_{k_1,k_2} \tilde{\psi}_{k_1} \tilde{\psi}_{k_2} \psi_{k_3} \psi_{-k_1-k_2-k_3} - 2N^{-2} \sum_{k_1,k_2} \omega_{k_1,0} \tilde{\psi}_{k_1} \psi_{k_2} \psi_{-k_1-k_2}. \quad (23)$$

We pause here to note some aspects of the model that are evident in this representation. The first is that the evolution operator L *contributes nothing* to the quadratic part of the action. (This can be seen immediately from Eq. (2): L is quartic in the fields.) Thus the resulting theory is nominally massless, and has *no evolution at all* in the Gaussian approximation, $\mathcal{L}_I = 0$. (Diffusion, in this model, is cooperative, requiring the presence of at least two particles at the same site.) The action, moreover, contains no parameters whatever, the relevant parameter p being "hidden" in the initial probability distribution. A further difference from continuum descriptions of more familiar processes such as DP[15,16] is that the order parameter is given by $\langle \psi^2 \rangle$ not $\langle \psi \rangle$.

2.3. Reorganized Action

In ref. 32 the path-integral representation serves as the basis for an expansion of the activity density in powers of time. We now show how the action derived above may be reorganized to generate an expansion of the *stationary* activity density $\rho_\infty \equiv \lim_{t\to\infty} \rho(t)$. As noted, we assume a Poisson-product initial distribution, with expectation p, for the occupation numbers n_i. Thus $\langle \psi_{k=0} \rangle = Np$, a constant of the motion, due to particle conservation. In the infinite-size limit, the law of large numbers implies that $N^{-1}\psi_{k=0}(t) = p$, and is no longer a random variable. We may therefore isolate all terms with $k = 0$ in Eq. (23) setting each factor $N^{-1}\psi_{k=0}$ equal to p. (Observe as well that $\tilde{\psi}_{k=0}$, the variable conjugate to $\psi_{k=0}$, is not required since $\psi_{k=0}$ is not random.) As a result of this procedure $\mathcal{G}[\psi, \tilde{\psi}]$ assumes the form

$$\mathcal{G}[\psi, \tilde{\psi}] \equiv \exp\left[-N^{-1} \int_0^t dt' \sum_{k\neq 0} (\tilde{\psi}_k \dot{\psi}_{-k} + \gamma_k \tilde{\psi}_{-k} \psi_k) + \int_0^t dt' \, \mathcal{L}_I' \right], \quad (24)$$

with

$$\gamma_k = 4\, p\, \omega_{-k,0} = 4\, p\, (1 - \cos k) \quad (25)$$

and the modified interaction

$$\begin{aligned}\mathcal{L}_I' = &-N^{-3}\sum_{k_1,k_2,k_3\neq 0}\omega_{k_3,-k_1-k_2-k_3}\psi_{k_1}\psi_{k_2}\tilde{\psi}_{k_3}\tilde{\psi}_{-k_1-k_2-k_3}\\ &-2pN^{-2}\sum_{k_1,k_2\neq 0}\omega_{k_2,-k_1-k_2}\psi_{k_1}\tilde{\psi}_{k_2}\tilde{\psi}_{-k_1-k_2}\\ &-2N^{-2}\sum_{k_1,k_2\neq 0}\omega_{-k_1-k_2,0}\psi_{k_1}\psi_{k_2}\tilde{\psi}_{-k_1-k_2}-p^2N^{-1}\sum_{k\neq 0}\omega_{k,-k}\tilde{\psi}_k\tilde{\psi}_{-k}.\end{aligned} \tag{26}$$

In Eq. (26) it is understood that none of the wavevectors associated with the fields ψ and $\tilde{\psi}$ may be zero.

The reorganized action differs from the original in certain important respects. The bilinear part $\mathcal{L}_0$ of the action in Eq. (24) represents independent diffusion of particles at rate $4p$.[41] (This can be seen by noting that the Markovian evolution operator for nearest–neighboring hopping at rate D is $L = D\sum_i[(1/2)\pi_{i-1} + (1/2)\pi_{i+1} - \pi_i]a_i$, which corresponds to $\mathcal{L} = -DN^{-1}\sum_k(1-\cos k)\hat{\psi}_{-k}\psi_k$.) The appearance of diffusion at rate $4p$ may be understood intuitively as follows. The rate of diffusion events at a given site is $n(n-1)$, i.e., twice the number of distinct pairs, so that the diffusion rate *per pair* is 2. The diffusion rate per particle is twice the diffusion rate per pair times the number of pairs per particle, or $4(n-1)\simeq 4n\simeq 4p$ if $p\gg 1$. Unlike the original representation of Eq. (22), the control parameter p now appears explicitly in the action. It is worth noting that this reorganization of the action is not readily implemented in the operator representation, Eq. (2), because in this case it is the *operator* $N^{-1}\sum_i \pi_i a_i$ that assumes a fixed value p.

3. PERTURBATION THEORY

Let Eq. (24) with $\mathcal{L}_I' \equiv 0$ define $\mathcal{G}_0$; Eq. (21) with $\mathcal{G}_0$ in place of $\mathcal{G}$ defines the free expectation $\langle\mathcal{A}\rangle_0$. Then for $k\neq 0$ we have[32] $\langle\psi_k(s)\rangle_0 = \langle\tilde{\psi}_k(s)\rangle_0 = 0$, and the basic contraction or propagator is

$$\langle\psi_{k'}(u)\tilde{\psi}_k(s)\rangle_0 = N\delta_{k',-k}\Theta(u-s)e^{-\gamma_k(u-s)}, \tag{27}$$

where Θ represents the step function. As usual in this formalism, $\Theta(0) = 0$.[41] The free expectation of n fields $\tilde{\psi}$ and n fields ψ is given by the sum of all possible products of n contractions.

The expectation of an observable may be written in the form

$$\langle \mathcal{A} \rangle = \left\langle \mathcal{A} e^{\int_0^t \mathcal{L}' \, dt'} \right\rangle_0, \tag{28}$$

which can be expressed in terms of free expectations if we expand the exponential. In this expansion, each field $\tilde{\psi}_k(\tau)$ must be contracted with a field $\psi_{-k}(\tau')$, with $\tau' > \tau$. At nth order there is a factor of $1/n!$ and integrations $\int dt_1 \cdots dt_n$ over the interval $[0, t]$. We impose the time ordering $t \geqslant t_1 \geqslant t_2 \geqslant \cdots \geqslant t_n \geqslant 0$, thereby cancelling the factor $1/n!$ We adopt a diagrammatic notation[32] in which fields $\psi(\tilde{\psi})$ are represented by lines entering (leaving) a vertex. All lines are directed to the left, the direction of increasing time. The first term in $\mathcal{L}_I'$, Eq. (26), corresponds to a vertex with four lines ("4-vertex"), the second and third to vertices with three lines ("3-vertex"), while the fourth, with two lines exiting, will be referred to as a "source." Figure 1 shows the vertices associated with $\mathcal{L}_I'$, as well as the "sink" corresponding to ρ. Vertex b will be called a "bifurcation" and c a "junction". In this way, the activity density

$$\rho = N^{-2} \sum_k \langle \psi_k \psi_{-k} \rangle = N^{-2} \sum_k \langle \psi_k \psi_{-k} \, e^{\int_0^t dt' \, \mathcal{L}_I'} \rangle_0 \tag{29}$$

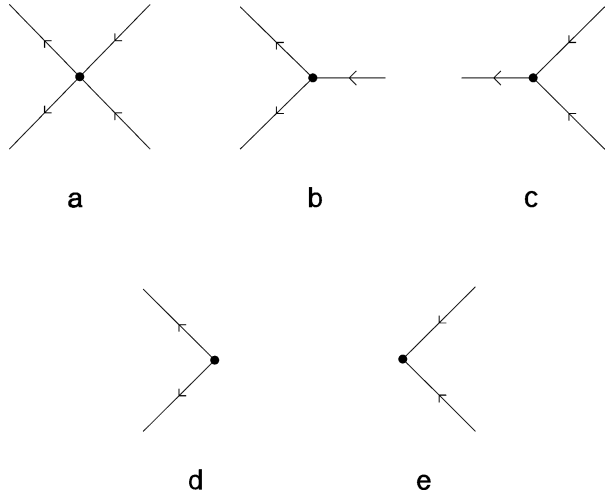

Fig. 1. Vertices (a–d) in the interaction $\mathcal{L}'$ and the sink (e) representing the activity density.

takes the form

$$\rho = N^{-2}\langle \psi_{k=0}^2 \, e^{\int_0^t dt' \, \mathcal{L}_I'} \rangle_0 + N^{-2} \sum_{k \neq 0} \langle \psi_k \psi_{-k} \, e^{\int_0^t dt' \, \mathcal{L}_I'} \rangle_0. \tag{30}$$

In the first term the only nonzero contribution is at zeroth order (no factors of $\mathcal{L}_I'$), and is equal to p^2, associated with the initial Poisson distribution. The second term generates an infinite set of diagrams; the zeroth order term vanishes since $\langle \psi_k \psi_{-k} \rangle = 0$ for $k \neq 0$.

Consider the first order diagram in the expansion. From Fig. 1 it is evident that the only vertex that can be contracted with the sink (without leaving dangling lines) is the source. This *simple loop*, shown as the first diagram on the right hand side of Fig. 2, makes the contribution

$$\begin{aligned} -2p^2 N^{-1} \sum_k \omega_{k,-k} \int_0^t e^{-2\gamma_k (t-t_1)} &= \frac{p}{4} \int_{-\pi}^{\pi} \frac{dk}{2\pi} (1 + \cos k)[e^{8p(1-\cos k)t} - 1] \\ &= \frac{p}{4} \left\{ e^{-8pt}[I_0(8pt) + I_1(8pt)] - 1 \right\}, \end{aligned} \tag{31}$$

where the prefactor 2 on the left hand side is a combinatorial factor and I_ν denotes the modified Bessel function. Here we used

$$N^{-1} \sum_k \overset{N \to \infty}{\longrightarrow} \int_{-\pi}^{\pi} \frac{dk}{2\pi}. \tag{32}$$

Thus this diagram yields the contribution identified in ref. 32 as $\rho_{\max}(t)$, the sum of all contributions at order t^n $(n = 1, 2, 3, ...)$ proportional to p^{n+1}, the highest power of p allowed at a given order. In the limit $t \to \infty$ the contribution to the activity from this term is $-p/4$. (As will be seen, all contributions to ρ coming from diagrams are of lower order in p than the zeroth-order term p^2.)

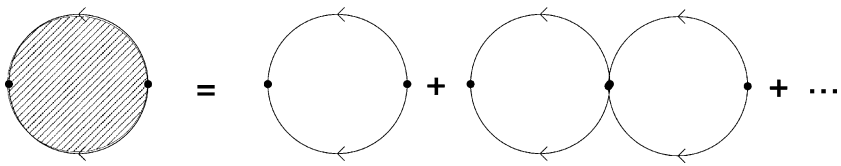

Fig. 2. Definition of a "dressed loop" as the sum of one, two, three,... simple loops joined at 4-vertices.

To study the stationary regime it is convenient to use the Laplace transform. For example, the Laplace transform of the contribution due to the simple loop, Eq. (31), is

$$-\frac{2p^2}{s}\int_{-\pi}^{\pi}\frac{dk}{2\pi}\frac{1-\cos^2 k}{s+8p(1-\cos k)}, \tag{33}$$

where s denotes the transform variable. Using the property $\lim_{t\to\infty} f(t) = \lim_{s\to 0} s\tilde{f}(s)$, we obtain the limiting contribution $-p/4$ directly.

Consider an arbitrary diagram D of n vertices, and denote the time-dependent factors in its contribution to $\rho(t)$ by $f_D(t)$. The Laplace transform of this contribution has the form

$$\begin{aligned}\tilde{f}_D(s) &= \int_0^\infty dt\, e^{-st}\int_0^t dt_1\int_0^{t_1} dt_2 \ldots \int_0^{t_{n-1}} dt_n e^{-\alpha_1(t-t_1)-\alpha_2(t_1-t_2)\ldots-\alpha_n(t_{n-1}-t_n)} \\ &= \int_{t_1}^\infty dt\int_{t_2}^\infty dt_1 \ldots \int_0^\infty dt_n e^{-(\alpha_1+s)(t-t_1)-(\alpha_2+s)(t_1-t_2)\ldots(\alpha_n+s)(t_{n-1}-t_n)-st_n} \\ &= [s(\alpha_1+s)(\alpha_2+s)\ldots(\alpha_n+s)]^{-1},\end{aligned} \tag{34}$$

where the α_i are functions of the wavevectors. Then we have

$$\bar{f}_D \equiv \lim_{t\to\infty} f_D(t) = \prod_{i=1}^{n}\frac{1}{\alpha_i}. \tag{35}$$

The factors α_i for diagram D may be determined by drawing vertical lines through each vertex of D. Then α_i is the sum of the factors γ_q for all propagators running between the vertical lines associated with vertices i and $i-1$ (here $t_0 \equiv t$), *regardless of whether or not these propagators link vertices* i and $i-1$.

For example, a diagram composed of n simple loops (see Fig. 2) makes a contribution of

$$\frac{(-1)^n 2^n p^2}{s}\left[\int_{-\pi}^{\pi} dk/2\pi\,\frac{1-\cos^2 k}{s+8p(1-\cos k)}\right]^n, \tag{36}$$

to $\tilde{\rho}(s)$, and so its contribution to ρ_∞ is

$$\frac{(-1)^n 2^n p^2}{(8p)^n} = (-1)^n p^2 \frac{1}{(4p)^n}. \tag{37}$$

Summing on n, we find the contribution due to this sequence of diagrams to the reduced activity $\bar{\rho} \equiv \lim_{t\to\infty}(\rho/p^2)$:

$$\sum_{n=1}^{\infty}\left(\frac{-1}{4p}\right)^n = -\frac{1}{1+4p} \equiv -\kappa. \tag{38}$$

In certain cases it is straightforward to replace a simple loop with the infinite sum of 1, 2, 3, ... loops. This procedure, illustrated graphically in Fig. 2, will be called *dressing* a loop.

Figure 3 shows a three-vertex diagram not included in the sequence represented by Fig. 2. It makes the following contribution to $\bar{\rho}$:

$$\frac{-32p}{4p(8p)^2}\int_{-\pi}^{\pi}\frac{dk}{2\pi}(1+\cos k)\int_{-\pi}^{\pi} dq/2\pi\,\frac{1-\cos q\,\cos(k-q)}{3-\cos q-\cos k-\cos(k-q)}. \tag{39}$$

The integral over wavevector q arises frequently in the diagrammatic series and can be evaluated in closed form

$$\begin{aligned} I(k) &= \int_{-\pi}^{\pi}\frac{dq}{2\pi}\,\frac{1-\cos q\,\cos(k-q)}{3-\cos q-\cos k-\cos(k-q)}. \\ &= \frac{1}{2}\left[\frac{3-c-\sqrt{(1-c)(7-c)}}{1+c}+\sqrt{\frac{1-c}{7-c}}\right], \end{aligned} \tag{40}$$

where c denotes $\cos k$.

In any diagram (beyond the set included in Fig. 2), we may insert any number of loops immediately to the right of the sink. That is, the sink may be replaced by a dressed loop. The same applies to the rightmost source, vertex n. The result is that the contribution of the original

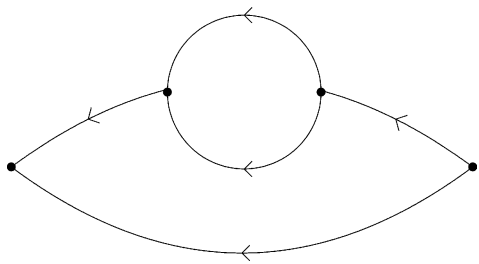

Fig. 3. A three-vertex diagram.

diagram is multiplied by $[4p/(1+4p)]^2$. Once this factor is included, no diagram with a 4-vertex immediately to the left of the rightmost source (i.e., in position $n-1$) or immediately to the right of the sink (position 1) need be included in the series.

4. DIAGRAMMATIC ANALYSIS

To begin we define the rules for constructing diagrams in the series for $\bar{\rho}$.[32] (Since there is exactly one factor of N^{-1} associated with each wavevector sum, all of the latter may be changed to integrals, using Eq. (32).)

1. Draw all connected diagrams of n vertices and a sink to the left of all vertices; the rightmost vertex must be a source. Each line exiting vertex j must be contracted with a line entering some vertex $i<j$. There is a factor $\delta_{k',-k}$ associated with each such contraction, where k is the wavevector exiting vertex j and k' the wavevector entering vertex i. The requirement that all lines be contracted leads to the condition $2(n_s-1)+n_b-n_c=0$, where n_s is the number of sources, n_b the number of bifurcations, and n_c is the number of junctions.

2. Each diagram possesses a factor of $(-1)^n$ and a combinatorial factor reflecting the number of ways of realizing the contractions. In the series for $\bar{\rho}$, this factor is given by 2^C, with $C=1+n_3+2n_4+n_s-\ell$, where n_3 is the number of 3-vertices (of either kind), n_4 the number of 4-vertices, and ℓ is the number of simple loops.

3. Associated with each bifurcation is a factor $2p\omega_{k_1,k_2}=2p[1-\cos k_1 \cos k_2]$. Each junction carries a factor $2\omega_{k,0}$ and each 4-vertex a factor ω_{k_1,k_2}. Each source carries a factor of $p^2\omega_{k,-k}$. (The k_i denote the wavevectors exiting the vertex.)

4. There is a factor $\bar{f}_D$ resulting from the time integrations, as discussed above.

5. Replace the sink and rightmost source with dressed loops, leading to the factor $[4p/(1+4p)]^2$ mentioned above, and exclude all diagrams with a 4-vertex in position 1 or $n-1$.

6. Integrate over all wavevectors.

Collecting the factors of p and $1/p$ associated with the various vertices, $\bar{f}_D$, and the factor of p^{-2} in the definition of $\bar{\rho}$, we find that each diagram in the series for $\bar{\rho}$ contains an overall factor p^{-r}, where $r=n-n_b-2(n_s-1)$. Using the relation $2(n_s-1)+n_b-n_c=0$, we have $r=n-n_c$.

In order to take advantage of our simple results for the sum of an infinite set of diagrams represented by the dressed loops, we adopt

$\kappa \equiv (1+4p)^{-1}$ as the expansion parameter rather than p. Noting that $4p/(1+4p) = 1-\kappa$, and that $1/p = 4\kappa/(1-\kappa)$, we see that the first order diagram (i.e., the single dressed loop of Fig. 2) carries a factor of $4/(1+4p) = 4\kappa$, while diagrams at higher order carry a factor $[4p/(1+4p)]^2$, so that at order $1/p^r$ there is an overall factor of $(4\kappa)^r/(1-\kappa)^{r-2}$. Thus for $r > 2$, diagrams $\propto 1/p^r$ contribute at order κ^r and at all higher orders. Diagrams $\propto 1/p^r$ must have at least $r+1$ vertices and no more than $3r-2$ vertices.

Enumeration of diagrams at a given order involves (1) identifying all allowable sequences of n vertices, and (2) identifying all possible sets of connections between vertices, for each sequence. For diagrams with $n \geqslant 3$ (i.e., those not included in the simple dressed loop of Fig. 2), vertex 1 (nearest the sink) must be a junction. (As explained above it cannot be a 4-vertex. If it were a bifurcation, the wavevector of the single line entering this vertex would of necessity be zero, but such terms have been excluded from the action.) For similar reasons, vertex $n-1$ must be either a source or a bifurcation. Once the vertex sequence has been fixed, all possible sets of contractions of outgoing and incoming lines must be enumerated. The single line exiting vertex 1 must, naturally, always terminate at the sink.

The enumeration of sequences and connections is readily codified in an algorithm that may be implemented via computer. In our algorithm, for each n and r, all possible vertex sequences (subject to the above limitations) are enumerated. Then all possible connections are generated, by simply running through all termination points for each line independently, and rejecting those choices that result in uncontracted lines. In the algorithm, a diagram is specified by its *bond set*. For a diagram with m lines, the bond set is given by the set of ordered pairs $\{(v_1, v_1'), ..., (v_m, v_m')\}$, where v_j' is the vertex from which line j emanates and $v_j < v_j'$ the vertex where it terminates. ($v_j = 0$ denotes the sink.) Thus the diagram of Fig. 3 can be written: (01) (12) (12) (23) (03). The algorithm was verified against hand enumeration up to third order.

Since the number of diagrams grows very rapidly, and each diagram corresponds to a multidimensional integral, we extended the routine to perform the wavevector integrations for each diagram generated. This entails construction of the numerator and denominator of the integrand, which are products of factors involving the cosines of various linear combinations of wavevectors. The numerator is a product of factors associated with each vertex, as noted in item 3 above. The denominator is a product of factors α_i associated with each interval between vertices. These factors are readily determined, given the vertex sequence and bond set, if the wavevectors associated with each line are suitably codified. Note that there is one free wavevector k_i associated with each vertex, except for

junctions, so that the number of wavevector sums is r. The wavevector exiting a junction is equal to the sum K of those entering. The lines exiting a source carry wavevectors k' and $-k'$. In the case of a bifurcation or a 4-vertex we may take the wavevectors of the lines exiting as k' and $K-k'$, where K denotes the wavevector entering (or the sum of the wavevectors entering, in the case of a 4-vertex). Thus we see that the construction of the integrand (including associated numerical factors) is a straightforward task that can also be realized in a computational algorithm. The integrals over the k_i are evaluated numerically using a midpoint method.[3] Based on results for varying numbers of intervals in the numerical integration, we are able to determine the coefficients with a relative uncertainty of 10^{-4} or less.

5. Results

We have carried out the expansion for $\bar{\rho}$ to order κ^4. Call the number of n-vertex diagrams at order $\kappa^r N_{n,r}$ and the contribution of this set of diagrams to the coefficient of $\kappa^r/(1-\kappa)^{r-2}$ in this series $b_{n,r}$; these values are reported in Table I.

The diagrammatic expansion yields the following expression for the stationary activity density

$$\bar{\rho}_\infty = 1-\kappa-1.788\,040\kappa^2-4.414\,481\kappa^3-14.632(2)\kappa^4+\mathcal{O}(\kappa^5), \qquad (41)$$

where the figure in parenthesis denotes a numerical uncertainty. In Fig. 4 we compare Eq. (41) against the results of a Monte Carlo simulation[33] using systems of up to 800 sites. (For each p value, simulations are performed for various system sizes and the results extrapolated to the infinite-size limit.) For $p \geqslant 3$ the difference between the series expression and simulation is less than 0.1%. In ref. 33, a similar degree of precision is obtained by extrapolating (using Padé approximants) a 16-term series (in powers of t) to the infinite-time limit. The present series of four terms appears to furnish (without transformation or extrapolation), information equivalent to that obtained from a much longer series in powers of t. It is worth noting that while the time series is divergent, the present series shows no evidence of being divergent for small values of κ. If we assume convergence for small κ, it is natural to interpret the first singularity on the positive-κ axis as marking the phase transition.

[3]The enumeration/integration code is available on request to the authors.

Table I. Numbers of Diagrams $N_{n,r}$ and Coefficients $b_{n,r}$ in the Expansion of the Activity for the One-Dimensional Sandpile

n	r	$N_{n,r}$	$b_{n,r}$
3	2	2	−2.384 052
4	2	3	0.596 013
4	3	4	5.625 989
5	3	49	−19.520 916
6	3	180	11.376 647
7	3	306	−1.896 110
5	4	8	−13.225 188
6	4	311	135.895 511
7	4	3 471	−311.353
8	4	21 961	256.075
9	4	76 261	−88.685
10	4	136 404	11.092

With a series of only four terms it is of course difficult to draw firm conclusions regarding the location of the critical point. We nevertheless analyze the series via Padé approximants.[44] The [2,2] approximant is the best behaved and is in excellent accord with simulation for $p \geqslant 1.5$. It yields a critical value of $p_c = 0.8677(3)$. (The [1,3] and [3,1] approximants give $p_c = 0.668$ and 0.702, respectively.) It is usual to analyse the Padé approximant to the series for the derivative of the logarithm of the order parameter ($d \ln \bar{\rho}/d\kappa$ in the present instance), as this function should exhibit a simple pole at the critical point. The [2,1] approximant does in fact give an improved estimate of $p_c = 0.9069$ (about 5% below the value found in simulations), while the [1,2] approximant yields $p_c = 0.860$. (A very similar result for p_c is obtained via Padé analysis of the 16-term time series.[33]) The residue at the pole of the [2,1] approximant is 0.198, well below any of the numerical estimates for the critical exponent β that have been reported, which suggest $\beta \simeq 0.4$.[24–26] For $p \geqslant 3$, the Padé expression and simulation agree to within uncertainty (see Fig. 4). (The relative uncertainty of the simulation result is 10^{-4}.)

The chief barrier to extending the series is the rapid growth in the cpu time required to evaluate the multiple integrals over wavevectors, combined with the explosive growth in the number of diagrams. (Enumeration of the diagrams represents a small faction of the computing time). Thus in the case of the stochastic sandpile the present approach does not appear viable beyond fourth order.

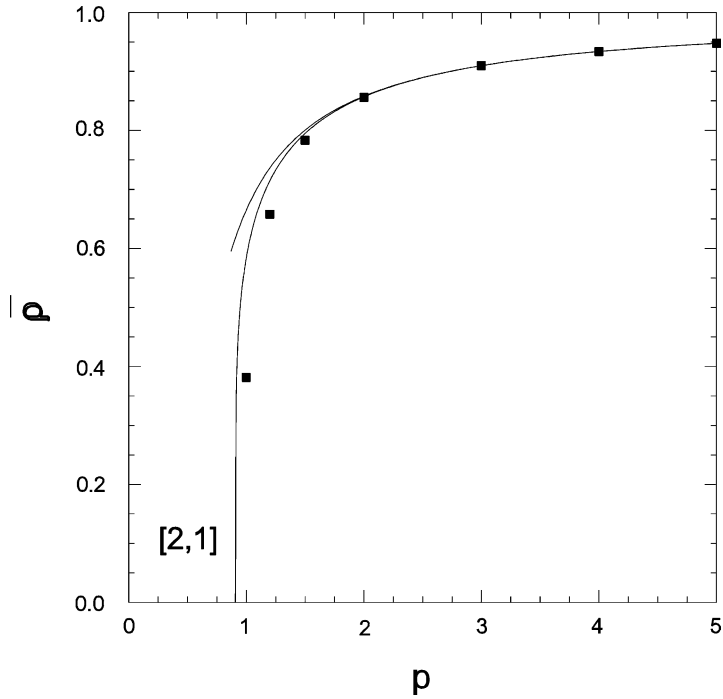

Fig. 4. Scaled stationary activity density $\bar{\rho}$ versus particle density p in one dimension. Upper curve: series prediction, Eq. (41); the curve labeled [2,1] is obtained by integrating the Padé approximant to the series for $d \ln \bar{\rho}/d\kappa$; points: Monte Carlo simulation. Error bars are smaller than the symbols.

For similar reasons the analysis of the two-dimensional case is restricted to $r \leqslant 3$. As explained in section 2.2, the formalism remains valid in d dimensions if we replace all factors $\omega_{k,k'}$ with $\omega_{\mathbf{k_1},\mathbf{k_2}}$ defined in Eq. (19). Thus γ_k in Eq. (25) becomes

$$\gamma_{\mathbf{k}} = 4\,p\,[1 - \lambda_d(\mathbf{k})] \tag{42}$$

with λ_d given by Eq. (20). The expansion involves the same set of diagrams in any dimension; only the integrals change, with the wavevectors now ranging over the first Brillouin zone in d dimensions.

In two dimensions our result for the stationary activity density is

$$\bar{\rho}_\infty = 1 - \kappa - 1.704\,155\kappa^2 - 3.7292\kappa^3 + \mathcal{O}(\kappa^4). \tag{43}$$

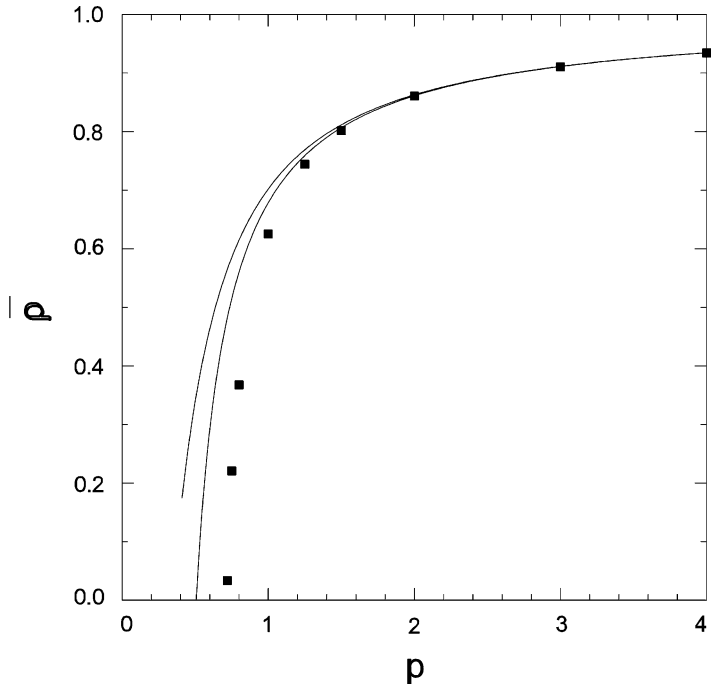

Fig. 5. Scaled stationary activity density $\bar{\rho}$ versus particle density p in two dimensions. Upper curve: series prediction, Eq. (43); lower curve: [2,1] Padé approximant to the series; points: Monte Carlo simulation.

The series prediction is compared against Monte Carlo simulation in Fig. 5; good agreement is observed for $p \geqslant 1.5$. The [2,1] and [1,2] Padé approximants to the three-term series for $\bar{\rho}$ yield critical values of $p_c = 0.507$ and 0.502, respectively, whereas the estimate from simulation is 0.715.

6. CORRELATION FUNCTIONS AND PROBABILITY DISTRIBUTION

Consider the stationary expectation $\langle n_j n_{j+\ell} \rangle$ of the product of occupations at sites j and $j+\ell$. For $\ell \neq 0$ this may be written as[32]

$$C(\ell) \equiv N^{-1} \sum_j \langle n_j n_{j+\ell} \rangle = N^{-2} \sum_k e^{ik\ell} \langle \psi_k \psi_{-k} \rangle \tag{44}$$

and separating the $k = 0$ term as in Eq. (30) we find

$$C(\ell) = p^2 + N^{-2} \sum_{k \neq 0} \cos k\ell \, \langle \psi_k \psi_{-k} e^{\int_0^t dt' \mathcal{L}_I'} \rangle_0. \tag{45}$$

The second term, an infinite sum of diagrams, defines the connected two-point correlation function $G(|\ell|)$. The lowest order contribution comes from the one-vertex diagram (simple loop) giving

$$G^{(1)}(|\ell|) = -\frac{p}{4}\int_{-\pi}^{\pi}\frac{dk}{2\pi}\cos k\ell\,(1+\cos k), \tag{46}$$

or $G^{(1)}(1) = -p/8$ and $G^{(1)}(|\ell|) = 0$ for $|\ell| > 1$. When the dressed loop is evaluated this becomes $G^{(1)}(1) = -\kappa p^2/8$. The correlation for sites separated by greater than unit distance is $\mathcal{O}(\kappa^2)$ or higher. From this result we can draw the following conclusions: (1) the nearest-neighbor correlation is negative for large p; (2) for large p correlations decay rapidly in space; (3) as $p \to \infty$, the reduced correlation $\bar{G}(\ell) = G(\ell)/p^2$ decays to zero (as $1/p$ or faster) so that in this limit the site occupancies are independent random variables.

The stationary expectation of $(\psi_j)^m$ (product of m fields at the same site) is related to the m-th factorial moment of the one-site occupation distribution. [For $m = 2$ this is seen explicitly in Eq. (13).] For $m = 3$ for example, we have

$$\langle n^3\rangle_F \equiv N^{-1}\sum_j \langle n_j(n_j-1)(n_j-2)\rangle = N^{-3}\sum_{k,k'}\langle\psi_k\psi_{k'}\psi_{-k-k'}\rangle, \tag{47}$$

which can be written

$$\langle n^3\rangle_F = p^3 + 3pN^{-2}\sum_{k\neq 0}\langle\psi_k\psi_{-k}\rangle + N^{-3}\sum_{k,k'\neq 0}\langle\psi_k\psi_{k'}\psi_{-k-k'}\rangle. \tag{48}$$

The second term equals $3p(\rho - p^2)$ and so is $\mathcal{O}(p^2)$ for large p. The third term must be expanded in diagrams with a three line sink. The lowest order diagram thus involves two vertices, a source and a bifurcation, and is $\mathcal{O}(p)$ for large p. We see then that $\langle n^3\rangle_F = p^3[1 + \mathcal{O}(1/p)]$ for large p. The same line of reasoning shows that the m-th factorial moment approaches p^m as $p \to \infty$. In this limit the one-site marginal distribution is therefore Poisson with parameter p, and by our previous result on independence, the joint probability distribution is a product of such distributions.

We defer a detailed analysis of correlation functions to future work, and stress that the main result of the present section is that in the large-p limit, the probability distribution is a product of identical Poisson distributions at each site, as was conjectured in ref. 33. It is readily seen that this remains valid in $d \geqslant 2$ dimensions.

7. DISCUSSION

We derive an expansion for the stationary activity density in a stochastic sandpile with a conserved particle density. Because of conservation, the $k = 0$ Fourier mode of the particle density (and the associated field ψ_k) has a fixed value, rather than being a random variable. This permits us to reorganize the action so that the control parameter p appears explicitly. The bilinear part of the action now describes diffusion at a rate $4p$. Because of this, the propagator carries an exponential factor, and all time integrations can be realized to obtain the limiting ($t \to \infty$) activity directly. The ensuing expansion for $\bar{\rho} = \lim_{t\to\infty} \rho(t)/p^2$ involves the parameter $\kappa = (1 + 4p)^{-1}$. We are able to sum certain infinite classes of diagrams through the device of "dressed loops." Despite this, the number of diagrams to be evaluated at each order grows explosively, so that our result extends only to $\mathcal{O}(\kappa^4)$ ($\mathcal{O}(\kappa^3)$ in two dimensions). The fourth-order series agrees very well with simulation in the supercritical regime, and yields (via Padé approximation) the critical value p_c to within about 5%. A similar favorable comparison is seen in the two-dimensional case, although the three-term series furnishes a poor estimate for p_c. Given these encouraging results, it is reasonable to hope that extended series will yield quantitative predictions for critical properties. In light of the complexities of the diagrammatic approach, a more promissing direction for such an extension may involve a direct operator expansion, as used in ref. 33 to extend the temporal series. We have also used the reorganized expansion to show that in the large-p limit, the sandpile is governed by a Poisson-product distribution. Our results strengthen the conclusion, based until now on simulation and mean-field-like analyses, that conserved sandpiles exhibit a phase transition as the particle density is varied. It is of great interest to know if the details of this transition can be analysed using the operator and path-integral formalisms.

ACKNOWLEDGMENTS

We are grateful to Miguel A. Muñoz for valuable comments on the manuscript. This work was supported by CNPq and CAPES, Brazil.

REFERENCES

1. P. Bak, C. Tang, and K. Wiesenfeld, *Phys. Rev. Lett.* **59**:381 (1987); *Phys. Rev. A* **38**:364 (1988).

2. D. Dhar, *Physica A* **263**:4 (1999) and references therein.
3. G. Grinstein, *Scale Invariance, Interfaces and Nonequilibrium Dynamics* (*NATO Advanced Study Institute, Series B: Physics, Vol. 344*) A McKane *et al.*, ed., (Plenum Press, New York, 1995).
4. D. Sornette, A. Johansen, and I. Dornic, *J. Physique I* **5**:325 (1995).
5. A. Vespignani and S. Zapperi, *Phys. Rev. Lett.* **78**:4793 (1997); A. Vespignani and S. Zapperi, *Phys. Rev. E* **57**:6345 (1998).
6. P. Bak, *How Nature Works* (Copernicus, New York, 1996).
7. Z. Olami, H. J. S. Feder, and K. Christensen, *Phys. Rev. Lett.* **68**:1244–1247 (1992).
8. T. P. Peixoto and C. P. C. Prado, *Phys. Rev. E* 69:025101 (2004).
9. R. Dickman, M. A. Muñoz, A. Vespignani, and S. Zapperi, *Braz. J. Phys.* **30**:27 (2000).
10. R. Dickman, *Physica A* **306**:90 (2002).
11. M. A. Muñoz *et al.*, Proceedings of the 6th Granada Seminar on Computational, in *Modeling Complex Systems*, J. Marro and P. L. Garrido, eds. AIP Conference Proceedings v. 574 (2001).
12. J. Marro and R. Dickman, *Nonequilibrium Phase Transitions in Lattice Models* (Cambrige University Press, Cambrige, 1999).
13. H. Hinrichsen, *Adv. Phys.* **49**:815 (2000).
14. See *Braz. J. Phys.* **30**:1 (2000).
15. H. K. Janssen, *Z. Phys. B* **42**:151 (1981).
16. P. Grassberger, *Z. Phys. B* 47:365 (1982).
17. G. Ódor, *Rev. Mod. Phys.* **20**:40 (2004).
18. P. K. Mohanty and D. Dhar, *Phys. Rev. Lett.* 89:104303 (2002).
19. A. Vespignani, R. Dickman, M. A. Muñoz, and S. Zapperi, *Phys. Rev. E* **62**:4564 (2000).
20. F. Bagnoli, F. Cecconi, A. Flammini, and A. Vespignani, *Europhys. Lett.* **63**:512 (2003).
21. M. Paczuski, S. Maslov, and P. Bak, *Europhys. Lett.* **27**:97 (1994).
22. A. Vespignani, R. Dickman, M. A. Muñoz, and S. Zapperi, *Phys. Rev. Lett.* **81**:5676 (1998).
23. F. van Wijland, *Phys. Rev. Lett.* **89**:190602 (2002).
24. R. Dickman, M. Alava, M. A. Muñoz, J. Peltola, A. Vespignani and S. Zapperi, *Phys. Rev. E* **64**:56104 (2001).
25. R. Dickman, T. Tomé, and M. J. de Oliveira, *Phys. Rev. E* **66**:16111 (2002).
26. S. Lübeck, *Phys. Rev. E* **65**:046150 (2002); *ibid* **66**:046114 (2002).
27. J. Kockelkoren and H. Chaté, eprint: cond-mat/0306039.
28. M. Rossi, R. Pastor-Satorras, and A. Vespignani, *Phys. Rev. Lett.* **85**:1803 (2000).
29. S. Lübeck and P. C. Heger, *Phys. Rev. Lett.* **90**:230601 (2003); *Phys. Rev. E* **68**:056102 (2003).
30. V. B. Priezzhev, E. V. Ivashkevich, A. M. Povolotsky, and C.-K. Hu, *Phys. Rev. Lett* **87**:84301 (2001).
31. S. Maslov and Y. C. Zhang, *Phys. Rev. Lett* **75**:1550 (1995).
32. R. Dickman and R. Vidigal, *J. Phys. A* **35**:7269 (2002).
33. J. Stilck, R. Dickman, and R. Vidigal, *J. Phys. A* **37**:1145 (2004).
34. M. Doi, *J. Phys. A* **9**:1465,1479 (1976).
35. R. Dickman, *J. Stat. Phys.* **55**:997 (1989).
36. R. Dickman and I. Jensen, *Phys. Rev. Lett.* **67**:2391 (1991).
37. I. Jensen and R. Dickman, *J. Stat. Phys.* **71**:89 (1993).
38. R. Dickman, J-S Wang, and I. Jensen, *J. Chem. Phys.* **94**:8252 (1991); M. J. de Oliveira, T. Tomé, and R. Dickman, *Phys. Rev. A* **46**:6294 (1992).
39. J. Zhuo, S. Redner, and H. Park, *J. Phys. A* **26**:4197 (1993).
40. L. Peliti, *J. Physique* **46**:1469 (1985).

41. R. Dickman and R. Vidigal, *Braz. J. Phys.* **33**:73 (2003).
42. S. S. Manna, *J. Phys. A* **24**:L363 (1991).
43. S. S. Manna, *J. Stat. Phys.* **59**:509 (1990).
44. G. A. Baker, *Quantitative Theory of Critical Phenomena* (Academic Press, New York, 1990).